RESEARCH PAPER

PCCP

www.rsc.org/pccp

B3LYP/6-31G* conformational landscape *in vacuo* of some pterocarpan stereoisomers with biological activity

Giuliano Alagona,* Caterina Ghio and Susanna Monti

CNR-IPCF, Molecular Modelling Lab, Via Moruzzi 1, I-56124 Pisa, Italy
E-mail: G.Alagona@ipcf.cnr.it; Fax: +39 050 3152442; Tel: +39 050 3152450

Received 25th November 2003, Accepted 6th January 2004
First published as an Advance Article on the web 28th January 2004

The relative stability of possible arrangements of the pterocarpan fused ring system and the conformational preferences of the side chains present in two natural compounds, 3,9-dimethoxy-4-prenylpterocarpan (bitucarpin A) and 3,9-dihydroxy-4,8-diprenylpterocarpan (erybraedin C), have been investigated *in vacuo* on a number of stereoisomers (either natural or not) at the B3LYP/6-31G* level. The results obtained using three classical force fields (Tripos/GH, MMFF94 and GAFF), compared to the quantum mechanical ones for selected torsions (hydroxyl and prenyl group rotations), indicate that MMFF94 produces a satisfactory description of structural features of pterocarpans, and thus it is advisable to resort to it when thorough *ab initio* or DFT investigations are not affordable. Two stable structures, named H_t and O_t from the substituent at the tetrahedral carbon vicinal to the chiral centre in *trans* position with respect to its H, have been found for the *cis* fused ring system, with H_t about 2 kcal mol^{-1} more favourable than O_t. The interconversion between H_t and O_t can occur along two pathways with distinct values of the dihedral angle between the benzofuran O and the *peri* C of chromane. For both stable skeleton arrangements there are a number of almost equivalent minima separated by considerably high barriers, in 3,9-dihydroxypterocarpan for the OH group rotations, and in bitucarpin A or in erybraedin C for the prenyl side chain rotations. For *trans* configurations, which are about 10 kcal mol^{-1} less favourable than *cis* configurations, only H_t arrangements have been located. In the case of erybraedin C, the structures obtainable by coupling on the two side chains in all possible ways the prenyl dihedral values related to minima in bitucarpin A have been studied with a single orientation of each hydroxy group. Starting from that hydroxy group arrangement, MMFF94 PES have been examined either for each minimum in the conserved prenyl chain or for changes in the second dihedrals while the first ones have been kept in the region of their minimum (both prenyl side chains almost perpendicular to the pterocarpan scaffold).

Introduction

Pterocarpans constitute the second largest group of natural isoflavonoids.[1] In contrast to flavonoids, natural isoflavonoids have a very limited distribution within the vegetable kingdom. They are present only in the Leguminosae family, mainly in the Papilionideae sub-family. Several isoflavonoid groups, including isoflavanones, isoflavones, isoflavanes as well as pterocarpans, are produced by plants in response to the intrusion of a disease-producing agent, such as bacteria, viruses or fungi.[1] Thus they are among the stress-induced metabolite constituents, acting as protective agents[2] (phytoalexins), of plants of the genus *Psoralea* common in the Mediterranean area as well as in the southern part of Africa, in North and South America and in Australia. Some of them have been used in ancient medicine for leucoderma (vitiligo) and for their potent antimicrobial activity.[3] In particular, a fraction has been extracted from *P. juncea* and *P. corylifolia* which showed, respectively, antimutagenic effects[4,5] and antitumoral activity.[3,6] Several weakly active topoisomerase II and DNA polymerase inhibitors have also been detected in a fraction of *P. corylifolia*,[7] whose seeds have been used as diuretic, stomachic and anthelmintic in Ayurvedic medicine,[8] and in traditional Native American healing practices.[4] Some pterocarpans have been reported to have antifungal,[9] antitubercolar and oestrogenic activity,[10] while others inhibit HIV-1 in cell cultures.[11] Two of them are antagonists against snake and spider venom,[12] although their mode of action is still to be explored. Since a wide number of synthetic routes, even stereoselective, to pterocarpans have been devised,[11b,13] unnatural pterocarpans, hopefully even more active than natural ones, could be synthesized. In order to do so, it is however necessary to preliminarily obtain a thorough insight of the conformational landscape of this class of compounds.

The main structural feature of pterocarpans consists in the simultaneous presence in their skeleton of two fused chromophores, 2,3-dihydrobenzo[*b*]furan and chromane, which give rise to two chiral centres (6a and 11a in Fig. 1). In this initial investigation carried out in the gas phase, we take into account the backbone structure and the conformational behaviour of the substituents (hydroxyl, methoxyl, and prenyl side chains) present in two pterocarpans extracted from *P. bituminosa* (so called because of its sharp bituminous smell when rubbed), a native herb in Italy known as "trifoglio cavallino" (*i.e.* horse shamrock), used formerly in popular medicine as an expectorant and as a vulnerary remedy[14] for its antiseptic and hemostatic properties. The two compounds, extracted among others and identified as bitucarpin A and erybraedin C,[15] also

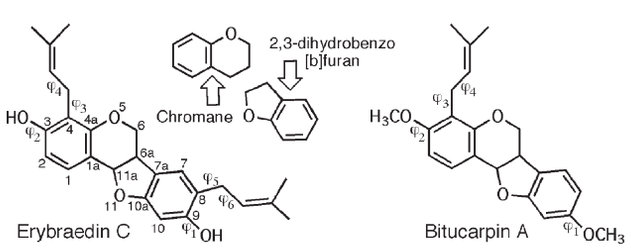

Fig. 1 Backbone structure, rotatable bonds and numbering of erybraedin C and bitucarpin A. The individual chromophores are also depicted.

DOI: 10.1039/b315234k

displayed in Fig. 1, have been shown to possess a distinct anti-cancer activity against colon solid tumours without appreciable cytotoxicity on human lymphocytes.[16]

Computational details

Geometry optimizations were carried out using the Gaussian 98 system of programs,[17] in the density functional theory (DFT) framework with B3LYP[18] (*i.e.* Becke's three parameter hybrid functional, LYP correlation functional) at the 6-31G* level.[19] Preliminary surface scans were performed at the Hartree–Fock (HF) level with limited basis sets (STO-3G[20] or 3-21G[21]). A few calculations were also carried out at the HF/6-31G* level for comparison. Stationary points were identified by frequency analysis at the B3LYP/6-31G* level. Thermal corrections for obtaining standard relative internal free energies, ΔG(int), for the conformers at $T = 298$ K and $p = 1$ atm were calculated using the rigid rotator–harmonic oscillator approximation.[22] Accordingly, ΔG(int) was calculated as

$$\Delta G(\text{int}) = \Delta E(0) + \Delta\text{ZPE} + \Delta\Delta H(0\text{–}T) - T\Delta\Delta S\,(0\text{–}T) \quad (1)$$

where the terms have the usual meaning: $\Delta E(0)$ is the quantum mechanical energy difference, while ΔZPE is the change in the vibrational energy at 0 K. The terms $\Delta\Delta H(0\text{–}T)$ and $\Delta\Delta S(0\text{–}T)$ stand for the relative changes in enthalpy and entropy from 0 to 298 K.

Tentative classical calculations, employing molecular mechanics (MM), used the GAFF force field within the AMBER7 framework[23] (partial charges have been determined with the RESP procedure[24] at the HF/6-31G* level) and the MMFF94[25] or Tripos/GH[26] force field within the SYBYL framework.[27]

Results and discussion

The fused ring scaffold, common to both compounds, was studied using as a model system 3,9-dihydroxypterocarpan, that corresponds to a completely deprenylated erybraedin C (with hydrogens replacing the prenyl side chains), before considering the conformational landscape arising from the rotatable bonds. Actually, despite the rigidity of fused rings, a limited conformational freedom is foreseeable within the skeleton itself, due to the presence of a CH_2 group at position 6, but not only to it as shown later on. Therefore, as a first step, the backbone structure was examined at the B3LYP/6-31G* level.

3,9-dihydroxypterocarpan

The *cis* (6a,11a) annulated structure, with O_{11} pseudo-axially oriented to avoid steric interaction with the *peri* C_1 hydrogen, is the most stable when one of the H at C_6 is *trans* with respect to the H at C_{6a}. The corresponding backbone structure is thus named H_t. When both H's at C_6 are *gauche* with respect to the H at C_{6a} (consequently O_5 is located in *trans*), the backbone structure (named O_t) is about 2 kcal mol^{-1} less favourable than the H_t one. In either case, the φ_1 ($=HOC_9C_{10}$) and φ_2 ($=HOC_3C_2$) torsions† produce four almost equivalent minima (see Table 1), not affected by the different backbone arrangements. As a matter of fact, the B3LYP/6-31G* stabilities are more sensitive to changes in φ_2 than in φ_1. When φ_2 is kept constant (either $=0°$ or 180°), the energy changes by 0.03 to 0.10 kcal mol^{-1} at most for opposite orientations of φ_1, whereas at φ_1 constant, for opposite orientations of φ_2, the changes are of the order of 0.20–0.27 kcal mol^{-1}.

† φ_1 and φ_2 have been defined such as to point both in the same direction (*i.e.* inward or outward) when they have the same value.

Table 1 B3LYP/6-31G* and MMFF94 relative stabilities[a] of the four local minima of 3,9-dihydroxypterocarpan depending on the OH groups arrangements[b]

Conformer	H_t		O_t	
φ_1,φ_2	B3LYP	MMFF94	B3LYP	MMFF94
0°,180°	0	0	0	0
180°,180°	0.078	0.727	0.109	0.759
0°,0°	0.249	0.480	0.274	0.595
180°,0°	0.287	1.082	0.309	1.128

[a] In kcal mol^{-1}. Reference energies for H_t and O_t are -879.696408 and -879.693309 E_h, respectively ($\Delta E = 1.94$ kcal mol^{-1}). [b] Roughly named 0° or 180° (DFT values always differ less than 1°).

In order to validate the behaviour of the empirical force fields taken into account in this study, potential energy profiles along the *cis–trans* (C–T) rotations in both directions of φ_1 (at $\varphi_2 = $ T) and φ_2 (at $\varphi_1 = $ C), obtained for the H_t structure, were compared with relevant B3LYP/6-31G* results (see Fig. 2).

The overall trend of quantum mechanical profiles is reproduced by the classical calculations, although Tripos/GH barriers are exceedingly low and GAFF minima for φ_1 or $\varphi_2 = $ T are not as stable as they should be. This effect is even more pronounced for φ_1 because in that case also φ_2 is trans. Among the force fields considered, MMFF94 gives the best performance. The relative stability of the local minima with the MMFF94 force field, also reported in Table 1, is fairly consistent with the B3LYP/6-31G* energy ordering (just the second and third minina are inverted), although energy gaps are in general somewhat higher than at the B3LYP/6-31G* level. The similarity between the φ_1 and φ_2 curves indicates that the OH group rotations are in general almost unaffected by the difference in the chemical composition of the closest chromophore to the rotating group.

For the sake of consistency with bitucarpin A (see below), which bears methoxy substituents, all geometry optimizations for 3,9-dihydroxypterocarpan, apart those involving OH group rotations, have been carried out starting from φ_1 and φ_2 values close to 0°, although this is not the lowest energy minimum for it. Moreover, this choice should not be in contrast with the possible outcome for erybraedin C, since in that case the OH group orientations likely depend on specific interactions of either each hydroxy hydrogen with the adjacent prenylic double bond *in vacuo* or H-bond donor/acceptor partners belonging to the environment in a protein or in solution.

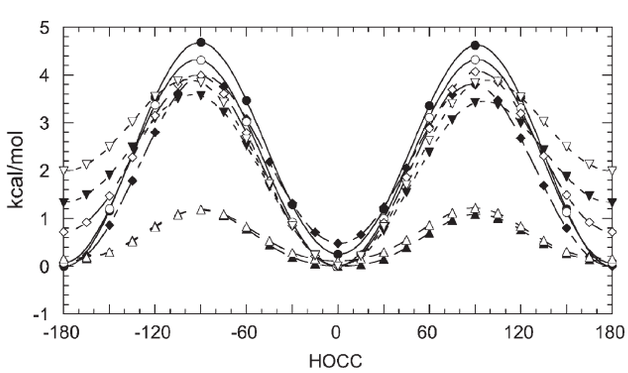

Fig. 2 GAFF (down triangles), MMFF94 (diamonds), Tripos/GH (up triangles) and B3LYP/6-31G* (circles) energy profiles for the C-T rotations of φ_1 (at $\varphi_2 = $ T, empty markers) and φ_2 (at $\varphi_1 = $ C, solid markers).

The two chromophores form a two-blade system, whose joint is along the C_{6a}–C_{11a} bond. In the H_t structure the angle between the blades is 145.3° (measured as the angle between the planes defined by $C_3C_{6a}C_{11a}$ and $C_{6a}C_{11a}C_9$) with the CH_2 group protruding inside, whereas in the O_t structure that angle is 100.5° with the CH_2 group outward, as can be seen in Fig. 3. As far as the $C_1C_{1a}C_{11a}O_{11}$ dihedral angle and the H_1–O_{11} separation are concerned, they are very close to each other (−65.4°/2.96 Å and −60.9°/2.89 Å, respectively) in H_t and O_t.

The standard projections of the six-membered O-heterocycle for the H_t and O_t structures in the *cis* (6aR,11aR) configuration, which was established since long,[28] are shown in the upper part of Scheme 1. Interestingly, the five-membered O-heterorings (lower part of Scheme 1), fused to the six-membered ones, have opposite helicity with respect to them.‡ These projections are particularly useful for the correlation between helicity and CD bands.[29] In this case, however, they have been displayed because they allow an immediate perception of the ring puckering, though decidedly enhanced.

H_t and O_t interconversion pathway

In order to evaluate the structure flexibility, the interconversion pathway between H_t and O_t was taken into account, starting from φ_1/φ_2 values near zero. Since during the interconversion the $O_5C_6C_{6a}C_{11a}$ dihedral angle (named β for short) should change sign, the TS was sought in the region where β is close to zero with the two Hs of the CH_2 group, respectively, below and above the ring plane. However, two different transition states, TS1 and TS2, respectively 6.27 and 6.81 kcal mol^{-1} above H_t, were located, depending on the initial structure chosen, as can be seen examining the flexible scan along β values −60° to 60° (or backward from 60° to −60°), displayed in Fig. 4.

Starting from the geometry where the forward and backward curves cross each other ($\beta \approx -3°$), a geometry very close to TS2 has been obtained from a QST2 calculation, whereas TS1 has been produced using the OPT = TS keyword. From a perusal of the geometrical parameters (some of them are reported for the stationary points in Table 2), only the $C_1C_{1a}C_{11a}O_{11}$ dihedral angle α, appreciably changed along the interconversion pathways, apart the scanned torsion and those related to it (*i.e.* $XC_6C_{6a}X$, with X = any adjacent atom). The potential energy surface (PES) was thus examined to clarify matters, using α and β as leading parameters. The relevant map, displayed in Fig. 5, shows two distinct paths joining the two minima for noticeably different values of α.

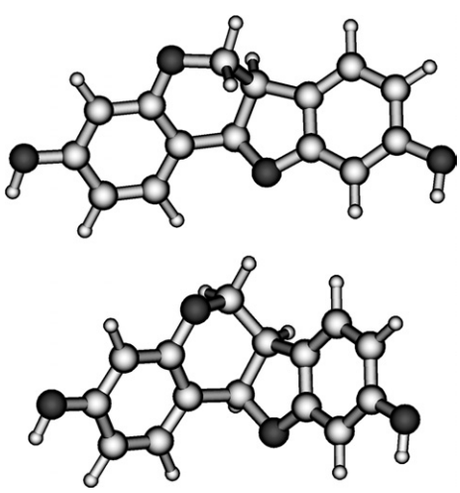

Fig. 3 Views of the B3LYP/6-31G* H_t (top) and O_t (bottom) structures of *cis* (6aR,11aR) 3,9-dihydroxypterocarpan.

‡ Obviously, the corresponding *cis* (6aS,11aS) H_t and O_t standard projections for both rings are the mirror images of the *cis* (6aR,11aR) ones; thus they have helicities opposite of those displayed in Scheme 1, but exactly the same energy.

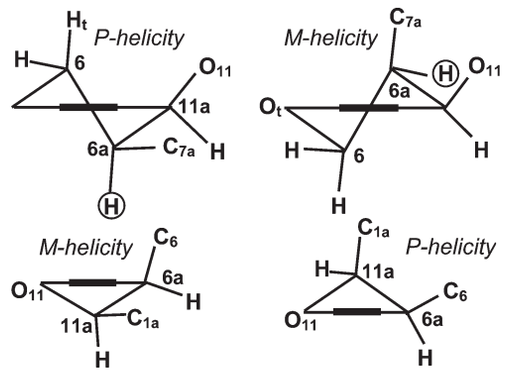

Scheme 1 Standard projections of heterorings in the H_t (left) and O_t (right) structures of *cis* (6aR,11aR).

The lowest energy path, surmounting the barrier at TS1, occurs for a decidedly pseudo-axial arrangement of O_{11} ($\alpha \approx -85°$, $\beta \approx -9°$), whilst the second saddle point, TS2, corresponds to $\alpha \approx -36°$ and $\beta \approx 12°$. Both structures are shown in Fig. 6. Despite the apparent strain in the ring structure due to the large value of α, TS1 is slightly more stable than TS2, probably because of its lower steric interaction with the *peri* C_1 H (H_1–O_{11} = 3.32 and 2.55 Å, respectively, in TS1 and TS2). The two blade systems are conserved at the transition states with almost insensitive changes in the angles between the blades (142.75° for TS1 and 99.65° for TS2). The CH_2 group is still inward in TS1 and outward in TS2 (Fig. 6). Thus the scaffold flexibility depends on both the presence of a CH_2 group and on its somewhat amazing capability of distortion about α by nearly 50°.

It is worth noticing that the interconversion coordinate does not coincide with either profile reported in Fig. 4. Those torsional profiles correspond to the lowest minimum along each PES section computed for fixed β values, unless a barrier is to be surmounted to reach it. In the latter case, the minimum closest to the starting geometry is located. Therefore roughnesses or hops along each profile indicate drifts from one path to the other, as can be verified by comparing the α values of adjacent points.

The orientation of the hydroxy groups does not affect the mutual stability of minimum and saddle point conformers, and their individual energies change by at most 0.3 kcal mol^{-1}.

3,9-dimethoxy-4-prenylpterocarpan (Bitucarpin A)

Once the skeleton arrangements were elucidated, a preliminary surface scan at the HF/STO-3G level has been carried out for

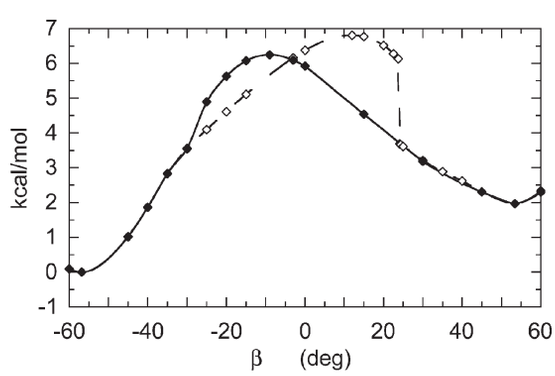

Fig. 4 B3LYP/6-31G* energy profile for the H_t/O_t interconversion. Forward (−60° to 60°, dashed line) and backward (solid line) directions.

Table 2 B3LYP/6-31G* torsional parameters of the H_t, O_t, TS1 and TS2 structures of 3,9-dihydroxypterocarpan

Parameter	H_t	O_t	TS1	TS2
$\beta = O_5C_6C_{6a}C_{11a}$	−56.8	53.4	−9.1	12.0
$O_5C_6C_{6a}H_{6a}$	64.5	173.6	112.3	132.7
$H_6C_6C_{6a}H_{6a}$	−174.2	51.6	−128.0	−104.8
$H_{6'}C_6C_{6a}H_{6a}$	−53.7	−68.0	−9.7	13.1
$C_6O_5C_{4a}C_{1a}$	−24.4	23.9	22.9	−26.4
$O_{11}C_{11a}C_{6a}C_6$	−93.5	−144.6	−93.9	−152.9
$C_{4a}C_{1a}C_{11a}C_{6a}$	−0.6	−2.5	−25.9	28.7
$C_{4a}O_5C_6C_{6a}$	55.3	−53.4	−17.0	18.6
$C_{1a}C_{11a}C_{6a}C_6$	29.2	−25.0	29.0	−33.5
$\alpha = C_1C_{1a}C_{11a}O_{11}$	−65.4	−60.9	−85.1	−36.2

bitucarpin A, in order to roughly evaluate the behaviour of its main degrees of freedom (shown in Fig. 1) in either case. Minima were found for φ_1 ($=COC_9C_{10}$) $\sim 0°$ or 180°, φ_2 ($=COC_3C_2$) $\sim 0°$, φ_3 ($=C_3C_4CC$) $\sim \pm 80°$ or $\pm 100°$, φ_4 ($=C_4CCC$) $\sim \pm 105°$. However, two leading parameters at most should be identified in order to perform an accurate investigation of the conformational landscape and the flexible scan of the PES. Since there was a slight preference (by ~0.2 kcal mol^{-1}) for structures with $\varphi_1 \sim 0°$, in the following, unless otherwise specified, the methoxy groups in position 3,9 were optimized starting from φ_1 and φ_2 values near 0°.

The PES for pairs of φ_3/φ_4 values (the two torsional degrees of freedom of the prenyl side chain) was therefore examined at the B3LYP/6-31G* level for either the H_t or O_t *cis* (6a,11a) structure, allowing all the other parameters to relax. The H_t maps, displayed in Fig. 7, show two couples of almost equivalent minima at $\varphi_3 \approx \pm 90°$ with $\varphi_4 \approx \pm 120°$, separated by a somewhat high ridge. As far as φ_3 is concerned, interestingly enough, a perpendicular arrangement of side chains with respect to dihydroxy substituted benzene (catechol) rings was found in the gas phase also for completely different systems, such as neurotransmitters (neutral/protonated dopamine[30] and protonated noradrenaline).[31] Even in the case of neutral analogs without OH groups on the aromatic ring, such as 1-amino-2-phenylethanol,[32] ephedrine ((1*R*,2*S*)-2-methylamino-1-phenylpropan-1-ol) and its 1*S*,2*S* stereoisomer, pseudoephedrine,[33] 2-phenylethyl alcohol and 2-phenylethylamine,[34] or in the presence of a methoxy substituent on the ring, as in *p*-methoxy phenethylamine,[35] the preferential arrangement of the side chain is *quasi* perpendicular, indicating that it is a common feature for this kind of substituted phenyl rings. A similar finding is reported also for tryptophan analogs, such as tryptamine,[36,37] and 3-indole-propionic acid.[36]

The O_t map, just shifted by ~1.95 kcal mol^{-1} with respect to the H_t one, when drawn taking its minimum as zero,

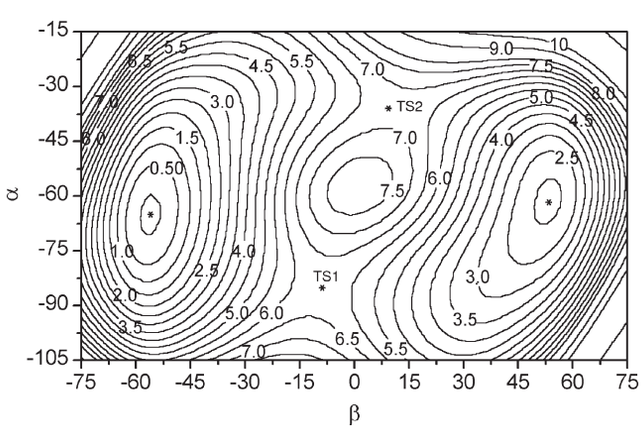

Fig. 5 B3LYP/6-31G* α–β PES for the H_t/O_t interconversion.

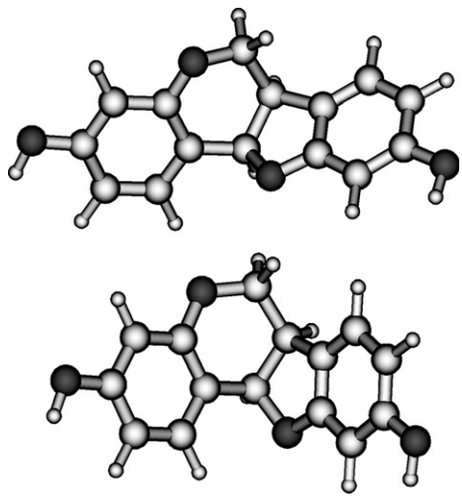

Fig. 6 Views of the B3LYP/6-31G* TS1 (top) and TS2 (bottom) structures of *cis* (6aR,11aR) 3,9-dihydroxypterocarpan.

looks almost exactly like the H_t one (rms = 0.38 kcal mol^{-1} considering all the grid points) and thus is not reported.

In order to identify a viable alternative to the expensive DFT calculations, the φ_3/φ_4 maps have also been computed with two classical force fields: Tripos/GH and MMFF94. The MMFF94 PES, shown in Fig. 8, is fairly similar, although somewhat steeper, to the B3LYP/6-31G* one. For the sake of comparison, isopotential contours spaced by 0.5 kcal mol^{-1} have been used below 5 kcal mol^{-1}, whereas above that value isopotential contours are spaced by 5 kcal mol^{-1}. In contrast, the Tripos/GH force field, whose PES is displayed in Fig. 9, produced eight different minima, slightly favouring conformers with $\varphi_3 > 180°$. In addition the regions of the minima were somewhat separated and located right below the peaks, which were conserved instead. The Tripos force field was thus abandoned.

The energy profiles in the $\varphi_3 \approx \pm 90°$ and $\varphi_4 \approx \pm 120°$ regions, depicted in Fig. 10, have been obtained by relaxing all the parameters but φ_4 or φ_3, respectively. They correspond, in this case, to the minimum energy paths due to the PES shape (Fig. 7), and thus φ_3 and φ_4 can significantly differ from ±90° and ±120° at least in the regions outside minima and TSs. The barriers for $\varphi_4 \approx 180°$ (1.5–1.6 kcal mol^{-1}) are about one third of those obtained for $\varphi_3 \approx 180°$ (4.7–4.9 kcal mol^{-1}, values explaining the out-of-plane orientation of the side chain). The structures of a choice of conformers (local minima and TSs) of bitucarpin A are shown in Fig. 11, while their relative energies, zero point energies, thermal corrections and relative free energies are reported in Table 3. Minima and lower energy TSs correspond to the out-of-plane arrangement of the prenyl side chain, whereas higher energy TSs are obtained for its in-plane arrangement. From a perusal of Table 3, it turns out that the mutual stability of the conformers does not change unless the free energy contribution is considered for the minima, which result to be reversed in their ordering. ZPE and thermal corrections somewhat reduce the internal energy barrier heights, whereas the free energy gap is enhanced. A word of caution is however necessary, because of the large number of low frequency modes explicitly taken as vibrations: some of them could be hindered rotations instead.

The *trans* stereoisomers have not been found in plants thus far. Nonetheless, it is interesting to examine their structural features, because synthetic methods are available also for them[13] and possibly they will soon be tested as antitumoral agents. Their backbone structure is remarkably different from the *cis* one, because the *trans* arrangement of the hydrogens at C_{6a}–C_{11a} introduces a considerable strain in the skeleton, which is somewhat twisted. The standard projections of the

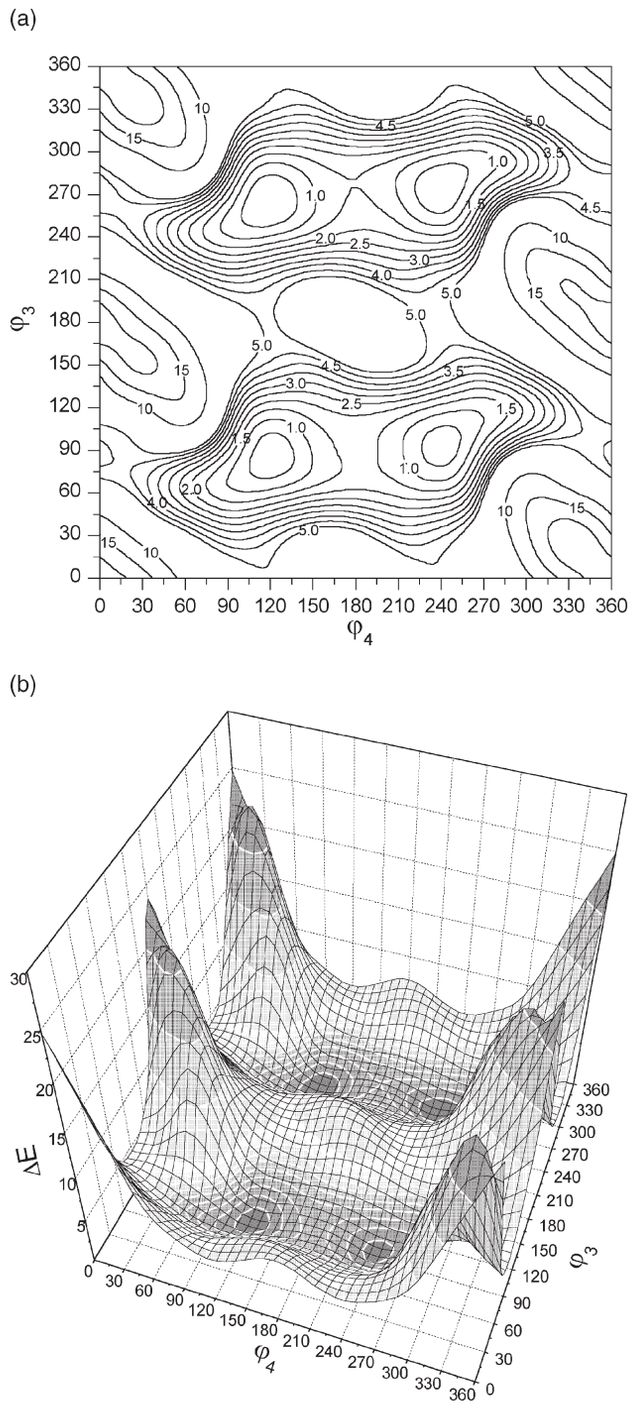

Fig. 7 B3LYP/6-31G* φ_3/φ_4 potential energy surface for H_t bitucarpin A.

heterorings for the *trans SR* and *RS* stereoisomers, displayed in Scheme 2, are mutual mirror images, as expected, and show that both rings have the same helicity, in contrast to the *cis* ones (see Scheme 1).

The *trans* stereoisomers are about 9.5 kcal mol^{-1} less stable than the corresponding *cis* stereoisomers. A similar gap ($\Delta\Delta H = 7.0$ and 11.7 kcal mol^{-1} with MMX and AM1, respectively) was obtained for an unsubstituted pterocarpan by Schöning and Friedrichsen in the first theoretical study on the stereochemistry of pterocarpanoids.[38] In that study, furthermore, the $\Delta\Delta H$ between the *cis* H_t and O_t structures, called there I and II after ref. 28, turned out to be 1.13 kcal mol^{-1}, in comparison to 1.94 and 1.95 kcal mol^{-1} obtained in this study at the B3LYP/6-31G* level for 3,9-dihydroxypterocarpan and bitucarpin A (3,9-dimethoxy-4-prenylpterocarpan). No O_t arrangement has been located for the *trans* stereoisomers, despite several trials have been carried out forcing firstly the backbone structure to relax with suitable constraints on the relevant dihedral angles.

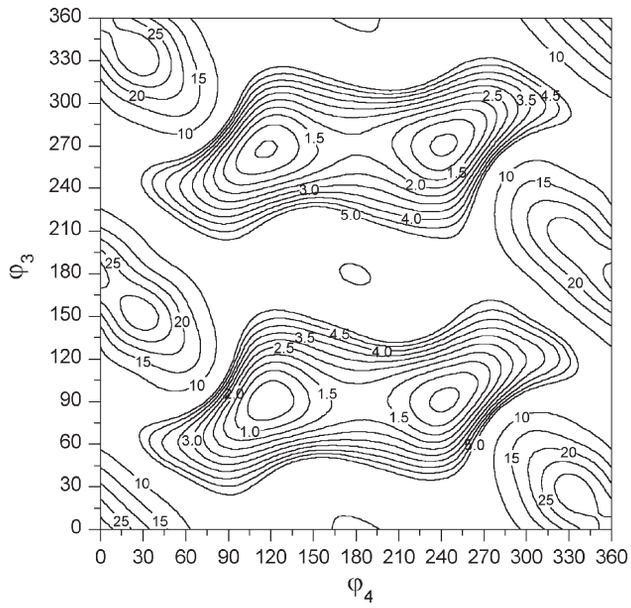

Fig. 8 MMFF94 φ_3/φ_4 potential energy surface for H_t bitucarpin A.

In Table 4 the torsional parameters for the side chains are reported for each minimum, indicated using its internal energy gap, on the φ_3/φ_4 PES for the H_t and O_t *cis* (6a*R*,11a*R*) and H_t *trans* (6a*R*,11a*S*) stereoisomers. As briefly discussed above, the methoxy groups prefer torsions close to zero, even in the absence of the steric hindrance due to the bulky prenyl group, although the energy difference between the $\varphi_1 \approx 0°$ and $\varphi_1 \approx 180°$ conformers is very limited (a few hundredths of a kilocalorie per mole at most).

3,9-dihydroxy-4,8-diprenylpterocarpan (Erybraedin C)

The situation is much more complicated for erybraedin C because of the presence not only of two prenyl side chains, but also of the hydroxy groups that, differently from the

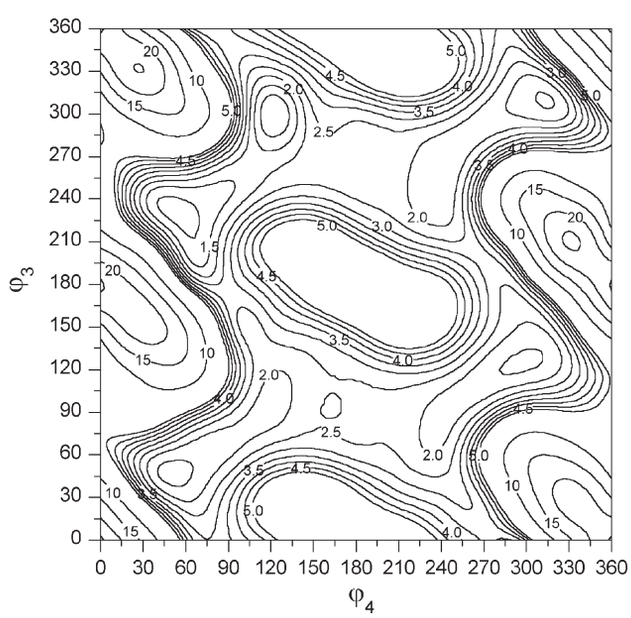

Fig. 9 Tripos/GH φ_3/φ_4 potential energy surface for H_t bitucarpin A.

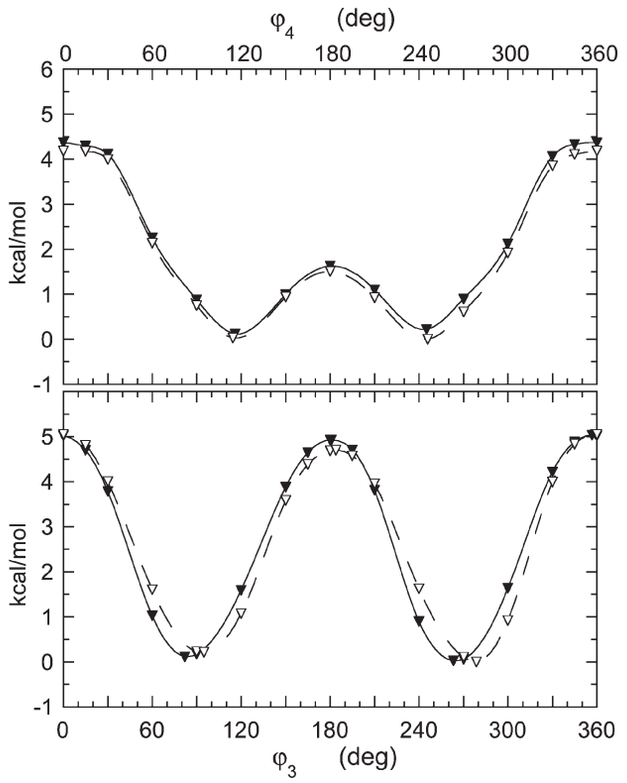

Fig. 10 B3LYP/6-31G* energy profiles for H_t bitucarpin A in the region about (top) $\varphi_3 \sim 90°$ (solid line) or $\varphi_3 \sim -90°$ (dashed line) and (bottom) $\varphi_4 \sim 120°$ (solid line) or $\varphi_4 \sim -120°$ (dashed line).

bitucarpin A methoxy groups, can interact with the prenylic π system. Therefore, rotations about the two prenyl side chains are to be considered, depending on the OH group orientations. In the working hypothesis that in a real environment (solvent or protein) they point outward, because the OH groups are involved in intermolecular interactions as proton donors (thus $\varphi_1 \approx \varphi_2 \approx 0°$), it is likely that the conformational minima of the prenyl side chains are consistent with those of bitucarpin A. Consequently, the sixteen possible combinations of the four minima for each prenyl group have been considered at the B3LYP/6-31G* level. As in the case of bitucarpin A, the

Table 3 B3LYP/6-31G* relative energies, zero point energies, thermal corrections and relative free energies[a] of stationary points on the PES of Fig. 7 in kcal mol^{-1}

ΔE	ΔZPE	ΔE_{th}	ΔH_{th}	ΔG
0	0	0	0	0.4047
0.0243	0.0207	0.0358	0.0351	0.3094
0.1142	0.0345	0.0809	0.0803	0.1406
0.2141	0.1732	0.2114	0.2114	0
1.5095	1.1358	0.7084	0.7078	2.0087
1.6252	1.2613	0.8302	0.8296	2.0237
4.7026	4.4359	3.8993	3.8987	6.1628
4.9284	4.7377	4.1817	4.1811	6.5939

[a] Each term includes all the previous ones, according to eqn. (1). Reference values (in E_h) are −1153.651967, −1153.234237, −1153.210248, −1153.209303, −1153.289693, in that order.

conformers turn out to have almost the same energy, reported in Table 5 together with the relevant values of the prenyl dihedral angles. The free energy difference, also reported in Table 5 for the $\varphi_3 \approx -97°$ and $\varphi_4 \approx 114°$ conformers only, is somewhat higher with an inversion in the ordering as well.

The MMFF94 φ_5 ($= C_7C_8CC$) and φ_6 ($= C_8CCC$) potential energy surfaces have been computed for each of the four φ_3,φ_4 minima in 30° steps. The PES for $\varphi_3 \approx -95°$ and $\varphi_4 \approx 114°$, shown in Fig. 12, exhibits four almost equivalent minima in couples slanting across. The two deepest minima ($\Delta E = 0$ and 0.12 kcal·mol^{-1} at $\varphi_3 = -95.3°$, $\varphi_4 = 112.9°$, $\varphi_5 = -93.2°$, $\varphi_6 = -112.1°$ and $\varphi_3 = -94.8°$, $\varphi_4 = 113.4°$, $\varphi_5 = 92.2°$, $\varphi_6 = 113.8°$ respectively) are along the main diagonal, while the other two minima ($\Delta E = 0.97$ and 0.98 kcal·mol^{-1} at $\varphi_3 = -95.8°$,$\varphi_4 = 113.4°$,$\varphi_5 = -92.1°$, $\varphi_6 = 114.8°$ and $\varphi_3 = -95.2°$,$\varphi_4 = 113.1°$,$\varphi_5 = 94.9°$,$\varphi_6 = -113.6°$ respectively) are along the secondary diagonal. The values in parenthesis have been obtained by subsequent mimization with MMFF94 in the regions of the minima. A similar shape is obtained also for the PES computed for the other three φ_3,φ_4 minima. Since the prenyl side chains are always almost perpendicular to the pterocarpan scaffold when $\varphi_1 \approx \varphi_2 \approx 0°$, PES at $\varphi_3 \approx \varphi_5 \approx \pm 90°$ have been computed for couples of φ_4,φ_6 values, still obtaining four minima at $\varphi_4 \approx \pm 120°$ and $\varphi_6 \approx \pm 120°$, with a slight preference for

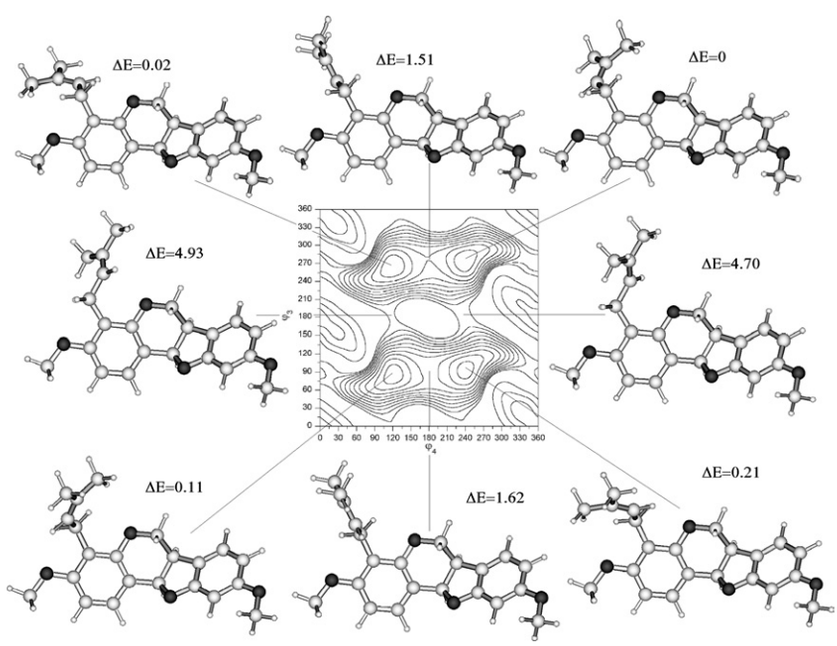

Fig. 11 B3LYP/6-31G* structures and relative energies (in kcal mol^{-1}) of local minima and TSs on the PES of *cis RR* bitucarpin A.

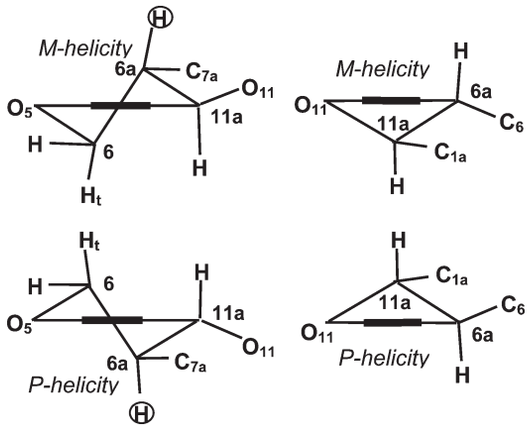

Scheme 2 Standard projections of heterorings in the 6a*S*,11a*R* (top) and 6a*R*,11a*S* (bottom) structures of *trans* bitucarpin A.

Table 4 B3LYP/6-31G* side chain torsional parameters (in °) of the low energy structures (in kcal mol^{-1}) for each bitucarpin A stereoisomer[a]

	Relative energy	φ_1	φ_2	φ_3	φ_4
RR H_t	0	−0.43	2.02	−81.42	−114.06
	0.024	−0.50	0.92	−96.86	114.35
	0.114	−0.83	−0.70	82.10	115.87
	0.214	−0.82	0.93	94.90	−114.97
RR O_t	1.951	−0.65	−0.12	96.33	−115.06
	1.953	−0.11	1.79	−84.18	−115.89
	2.004	−0.28	−1.13	79.81	112.62
	2.123	0.06	0.45	−95.49	115.14
SR H_t	9.509	−0.90	−1.53	82.49	115.19
	9.513	−1.04	−0.09	−97.82	113.45
	9.513	−0.93	0.99	−81.95	−115.41
	9.547	−0.86	−0.61	95.91	−115.57

[a] Dihedral values for the corresponding *SS* or *RS* stereoisomers are opposite in sign

$\varphi_6 \approx 120°$ at $\varphi_3 \approx \varphi_5 \approx 90°$ and $\varphi_6 \approx -120°$ at $\varphi_3 \approx \varphi_5 \approx -90°$. Whichever the φ_6 value, there is a secondary preference for $\varphi_4 \approx 120°$ at $\varphi_3 \approx \varphi_5 \approx 90°$ and for $\varphi_4 \approx -120°$ at $\varphi_3 \approx \varphi_5 \approx -90°$. In any case, the least stable regions are found in the corners (*i.e.* when φ_4 and φ_6 are close to 0° or 360°) with potential energy values slightly greater than 10 kcal mol^{-1}.

HF/6-31G* *vs.* B3LYP/6-31G*

In order to evaluate the effect of correlation corrections, a few calculations have been carried out at the HF/6-31G* level for comparison. The HF results, reported in Table 6, should be compared for H_t with the B3LYP/6-31G* ones reported in the upper left section of Table 5. For O_t the relevant B3LYP results are also reported in Table 6 (bottom). No sensitive difference appears in HF/6-31G* and B3LYP/6-31G* descriptions, either in the structures or in the relative energies. The largest HF/6-31G* energy gaps among the various minima were 0.026 and 0.033 kcal mol^{-1} for *cis* H_t and O_t, respectively, as compared to 0.047 and 0.068 kcal mol^{-1} obtained at the B3LYP/6-31G* level, with some changes in the ordering. The variety in the prenyl side chain positions corresponds to structures with the same energy as can be argued by the small energy differences obtained. Interestingly enough, the difference between the H_t and O_t structures is maintained for all the compounds and at all levels taken into account in this investigation.

Of course, only structures with for $\varphi_1 \approx \varphi_2 \approx 0°$ have been considered in this investigation. Several other arrangements of the OH groups as well as intermolecular H-bonds between them and a cluster made up of two water molecules at least should be taken into account to evaluate the electronic effects involved. These calculations are in progress and will be the subject of a forthcoming paper.[39]

Conclusions

The *cis* fused ring backbone of pterocarpans exhibits two different arrangements, named H_t and O_t depending on which atom at position 6 is *trans* with respect to H_{6a}. At the B3LYP/6-31G* level the H_t structure is about 2 kcal mol^{-1} more favourable than the O_t one, regardless nature and number of substituent groups. The pterocarpan skeleton constitutes a two-blade system with considerably different values of the angles between the blades in H_t (∼145°) and O_t (∼100°). The interconversion between the H_t and O_t structures occurs along two pathways with barrier heights of about 6–7 kcal mol^{-1}. The flexibility of the fused ring system is due to the presence of a CH_2 group in one of the rings and to the capability of the $C_1C_{1a}C_{11a}O_{11}$ dihedral angle to distort itself although belonging to a ring.

The OH groups in 3,9-dihydroxypterocarpan can assume almost equivalent coplanar orientations (φ_1 or φ_2 either close to 0° or 180°). In bitucarpin A, since the methoxy group vicinal to the prenyl side chain is anti with respect to C_4 to relieve the steric hindrance, an analogous orientation has been chosen for the other hydroxy group ($\varphi_1 \approx \varphi_2 \approx 0°$). The potential energy surfaces obtained for H_t and O_t show four minima with nearly equal stability separated by considerably high barriers for the interconversion between +anticlinal and −anticlinal arrangements of the prenyl side chain with respect to the pterocarpan scaffold. Conversely, the second dihedral along the prenyl side chain can vary from 120° to 240° across a barrier by about 1.5 kcal mol^{-1}. The prenyl chain torsional parameters are well conserved regardless the skeleton is *cis* (either H_t or O_t) or

Table 5 B3LYP/6-31G* relative energies and prenyl torsional parameters of the *cis* (6aR,11aR) H_t erybraedin C (for $\varphi_1 \approx \varphi_2 \approx 0°$) minima. Relative free energies are also reported for the lowest internal energy conformers[a]

ΔE	ΔG	φ_3	φ_4	φ_5	φ_6	ΔE	φ_3	φ_4	φ_5	φ_6
0	0	−97.94	113.89	81.48	−118.53	0.159	82.96	115.79	81.15	−118.85
0.025	0.373	−97.19	113.76	−81.78	118.78	0.160	82.01	115.23	−82.08	117.90
0.033	0.114	−96.20	114.63	79.98	120.78	0.191	81.59	114.55	79.76	119.35
0.047	0.194	−97.48	113.37	−79.59	−120.08	0.223	83.78	116.04	−80.63	−121.27
0.073		−83.02	−114.82	81.96	−118.74	0.171	96.01	−114.36	82.23	−118.70
0.125		−81.30	−113.94	−81.71	118.63	0.175	94.92	−114.43	−81.86	118.52
0.095		−80.92	−113.02	80.32	120.93	0.187	97.67	−112.80	79.58	119.71
0.113		−83.00	−114.63	−80.70	−120.56	0.204	97.59	−113.27	−80.28	−120.61

[a] In kcal mol^{-1} and °, respectively. The reference energy and free energy are −1270.382711 and −1269.965519 E_h, respectively.

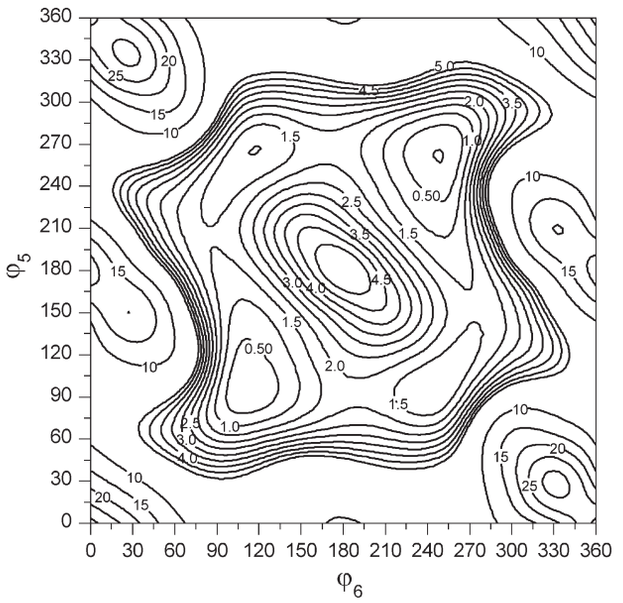

Fig. 12 MMFF94 φ_5/φ_6 potential energy surface for the $\varphi_3 \approx -90°$ and $\varphi_4 \approx 120°$ *cis* (6aR,11aR) erybraedin C.

Table 6 HF and B3LYP/6-31G* stabilities and torsional parameters of low energy structures for some *cis* erybraedin C conformers[a]

	Relative energy	φ_3	φ_4	φ_5	φ_6
RR H_t	0.005	−95.76	117.70	82.77	−120.87
HF	0.026	−93.76	117.69	−82.70	120.84
	0.003	−95.75	117.70	81.96	121.67
	0	−95.76	117.69	−82.13	−121.79
RR O_t	1.902	−95.17	118.42	−82.69	120.84
HF	1.875	−95.14	118.44	−82.07	−122.04
	1.883	−95.27	118.52	82.82	−121.03
	1.908	−95.82	118.40	81.95	121.20
RR O_t	1.939	−94.62	115.05	−82.43	118.72
B3LYP	1.977	−96.42	114.90	−79.92	−119.51
	1.993	−95.82	114.95	83.51	−117.67
	2.007	−96.84	114.86	79.53	118.86

[a] In kcal mol^{-1} and degrees, respectively. The HF/6-31G* reference energy is −1262.423510 E_h.

trans. Only H_t structures have been located for *trans* fused ring scaffolds, which are about 10 kcal mol^{-1} less stable than the *cis* H_t ones.

The behaviour of the GAFF (with HF/6-31G* RESP charges) and MMFF94 force fields turned out to be satisfactory for these systems, whereas the Tripos/GH force field produced a different pattern for the minima although in a similar region.

A limited exploration of the conformational preferences of erybraedin C has been carried out with a single orientation of both hydroxy groups ($\varphi_1 \approx \varphi_2 \approx 0°$). The preferential arrangements of the prenyl side chain are maintained in either positions (4 or 8).

By comparing the B3LYP and HF results, computed for a number of cases, the 6-31G* structures and energies are similar whether or not correlation corrections have been taken into account.

Acknowledgements

The authors are grateful to Dr Gino Turchi of the CNR Institute of Biophysics (Area della Ricerca di Pisa-San Cataldo) for stimulating their interest in these systems. S. Monti thanks James W. Caldwell for granting her permission to use AMBER7.

References

1 P. M. Dewick, "*Isoflavonoids*". In: *The Flavonoids: Advances in Research since 1980*, ed. J. B. Harborne, Chapman & Hall, London, 1988, pp. 125–204; P. M. Dewick, in: *The Flavonoids: Advances in Research since 1986*, ed. J. B. Harborne, Chapman & Hall, London, 1994, pp. 166–180.
2 P. M. Dewick and M. J. Steel, *Phytochemistry*, 1982, **21**, 1599.
3 P. G. Latha, D. A. Evans, K. R. Panikkar and K. K. Jayavardhanan, *Fitoterapia*, 2000, **71**, 223.
4 L. A. Mitscher, H. Telikepall, E. McGhee and D. M. Shankel, *Mutat. Res.*, 1996, **350**, 143.
5 S. R. Menon, V. K. Patel, L. A. Mitscher, P. Shih, S. P. Pillai and D. M. Shankel, *J. Nat. Prod.*, 1999, **62**, 102.
6 Y. M. Yang, J. W. Hyun, M. S. Sung, H. S. Chung, B. K. Kim, W. H. Paik, S. S. Kang and J. G. Park, *Planta Med.*, 1996, **62**, 353; P. G. Latha and K. R. Panikkar, *Fitoterapia*, 1998, **69**, 451.
7 N. J. Sun, S. H. Woo, J. M. Cassady and R. M. Snapka, *J. Nat. Prod.*, 1998, **61**, 362.
8 P. G. Latha and K. R. Panikkar, *J. Ethnopharmacol.*, 1999, **68**, 295; L. M. Perry, *Medicinal Plants of East and Southeast Asia: Attributed Properties and Uses*, MIT Press, MA, 1980, p. 223.
9 G. A. Lane, O. R. W. Sutherland and A. R. Skipp, *J. Chem. Ecol.*, 1987, **13**, 771.
10 C. R. Perrin and I. A. M. Cruickshank, *Phytochemistry*, 1969, **8**, 971.
11 T. A. Engler, O. K. Lynch, J. P. Reddy and G. S. Gregory, *Bioorg. Med. Chem. Lett.*, 1993, **3**, 1229; T. A. Engler, K. O. LaTessa, R. Iynegar, W. Chai and K. Agrios, *Bioorg. Med. Chem. Lett.*, 1996, **4**, 1755.
12 M. Nakagawa, K. Nakanishi, L. L. Darko and J. A. Vick, *Tetrahedron Lett.*, 1982, **23**, 3855.
13 L. Juhász, L. Szilágyi, S. Antus, J. Visy, F. Zsila and M. Simonyi, *Tetrahedron*, 2002, **58**, 4261; L. Kiss, L. Szilágyi and S. Antus, *Z. Naturforsch.*, 2002, **57b**, 1165; L. Kiss, T. Kurtán, S. Antus and A. Bényei, *Chirality*, 2003, **15**, 558; L. Kiss, T. Kurtán, S. Antus and H. Brunner, ARKIVOC 2003, http://www.arkat-usa.org/ark/journal/2003/Bernath/GB-653J/GB-653J.pdf and refs. quoted therein.
14 L. Fenaroli, *Flora Mediterranea*, Giunti, Firenze, 1998, p. 236.
15 L. Pistelli, C. Noccioli, G. Appendino, F. Bianchi, O. Sterner and M. Ballero, *Phytochemistry*, 2003, **64**, 595.
16 T. Maurich, *In vitro Study of the Activity of two Novel Compounds Extracted from Psoralea bituminosa on Cancer Cell-Lines and Human Lymphocytes*, 2002–2003 Thesis, University of Pisa.
17 M. J. Frisch, G. W. Trucks, H. B. Schlegel, G. E. Scuseria, M. A. Robb, J. R. Cheeseman, V. G. Zakrzewski, J. A. Montgomery, R. E. Stratmann, J. C. Burant, S. Dapprich, J. M. Millam, A. D. Daniels, K. N. Kudin, M. C. Strain, O. Farkas, J. Tomasi, V. Barone, M. Cossi, R. Cammi, B. Mennucci, C. Pomelli, C. Adamo, S. Clifford, J. Ochterski, G. A. Petersson, P. Y. Ayala, Q. Cui, K. Morokuma, D. K. Malick, A. D. Rabuck, K. Raghavachari, J. B. Foresman, J. Cioslowski, J. V. Ortiz, B. B. Stefanov, G. Liu, A. Liashenko, P. Piskorz, I. Komaromi, R. Gomperts, R. L. Martin, D. J. Fox, T. Keith, M. A. Al-Laham, C. Y. Peng, A. Nanayakkara, C. Gonzalez, M. Challacombe, P. M. W. Gill, B. G. Johnson, W. Chen, M. W. Wong, J. L. Andres, M. Head-Gordon, E. S. Replogle and J. A. Pople, *Gaussian 98 (Revision A.6)*, Gaussian, Inc., Pittsburgh, PA, 1998.
18 A. D. Becke, *J. Chem. Phys.*, 1993, **98**, 5648; C. Lee, W. Yang and R. G. Parr, *Phys. Rev. B*, 1988, **37**, 785.
19 R. Ditchfield, W. J. Hehre and J. A. Pople, *J. Chem. Phys.*, 1971, **54**, 724; W. J. Hehre, R. Ditchfield and J. A. Pople, *J. Chem. Phys.*, 1972, **56**, 2257; J. D. Dill and J. A. Pople, *J. Chem. Phys.*, 1975, **62**, 2921; P. C. Hariharan and J. A. Pople, *Theor. Chim. Acta*, 1973, **28**, 213.
20 W. J. Hehre, R. F. Stewart and J. A. Pople, *J. Chem. Phys.*, 1969, **51**, 2657.
21 J. S. Binkley, J. A. Pople and W. J. Hehre, *J. Am. Chem. Soc.*, 1980, **102**, 939.
22 D. A. McQuarrie, *Statistical Mechanics*, University Science Books, Sausalito, CA, 2000.
23 D. A. Case, D. A. Pearlman, J. W. Caldwell, T. E. Cheatham III, J. Wang, W. S. Ross, C. L. Simmerling, T. A. Darden,

K. M. Merz, R. V. Stanton, A. L. Cheng, J. J. Vincent, M. Crowley, V. Tsui, H. Gohlke, R. J. Radmer, Y. Duan, J. Pitera, I. Massova, G. L. Seibel, U. C. Singh, P. K. Weiner and P. A. Kollman, *AMBER7*, University of California, San Francisco, 2002.

24 C. I. Bayly, P. Cieplak, W. D. Cornell and P. A. Kollman, *J. Phys. Chem.*, 1993, **97**, 10 269.

25 T. A. Halgren, *J. Comput. Chem.*, 1996, **17**, 490; T. A. Halgren, *J. Comput. Chem.*, 1996, **17**, 520; T. A. Halgren, *J. Comput. Chem.*, 1996, **17**, 553; T. A. Halgren and R. B. Nachbar, *J. Comput. Chem.*, 1996, **17**, 587; T. A. Halgren, *J. Comput. Chem.*, 1996, **17**, 616.

26 J. Gasteiger and M. Marsili, *Tetrahedron*, 1980, **36**, 3219; J. Gasteiger and H. Saller, *Angew. Chem., Int. Ed. Engl.*, 1985, **24**, 687; E. Hückel, *Z. Phys.*, 1932, **76**, 628.

27 *SYBYL Molecular Modelling Software, Version 6.9 (Linux_os2)*, TRIPOS Associates, St. Louis, MO, April 2003.

28 K. G. R. Pachler and W. G. E. Underwood, *Tetrahedron*, 1967, **23**, 1817.

29 S. Antus, T. Kurtán, L. Juhász, L. Kiss, M. Hollósi and Zs. Májer, *Chirality*, 2003, **15**, 558.

30 G. Alagona and C. Ghio, *Chem. Phys.*, 1996, **204**, 239; P. I. Nagy, G. Alagona and C. Ghio, *J. Am. Chem. Soc.*, 1999, **121**, 4804.

31 G. Alagona and C. Ghio, *Int. J. Quantum Chem.*, 2002, **90**, 641; P. I. Nagy, G. Alagona, C. Ghio and K. Takács-Novák, *J. Am. Chem. Soc.*, 2003, **125**, 2770.

32 R. J. Graham, R. T. Kroemer, M. Mons, E. G. Robertson, L. Snoek and J. P. Simons, *J. Phys. Chem. A*, 1999, **103**, 9706.

33 P. Butz, R. T. Kroemer, N. A. Macleod and J. P. Simons, *J. Phys. Chem. A*, 2001, **105**, 544.

34 J. A. Dickinson, M. R. Hockridge, R. T. Kroemer, E. G. Robertson, J. P. Simons, J. McCombie and M. Walker, *J. Am. Chem. Soc.*, 1998, **120**, 2622.

35 I. Unamuno, J. A. Fernández, A. Longarte and F. Castaño, *J. Phys. Chem. A*, 2001, **105**, 11 524.

36 J. R. Carney and T. S. Zwier, *Chem. Phys. Lett.*, 2001, **341**, 77.

37 J. R. Carney and T. S. Zwier, *J. Phys. Chem. A*, 2000, **104**, 8677.

38 A. Schöning and W. Friedrichsen, *Z. Naturforsch. B*, 1989, **44**, 975.

39 G. Alagona and C. Ghio, work in progress.